Effect of cascade overlap and C15 clusters on the damage evolution in Fe : An OKMC study

Esfandiarpour, A.

2022-03

Esfandiarpour , A , Byggmästar , J , Balbuena , J P , Caturla , M J , Nordlund , K & Granberg , F 2022 , ' Effect of cascade overlap and C15 clusters on the damage evolution in Fe : An OKMC study ' , Materialia , vol. 21 , 101344 . https://doi.org/10.1016/j.mtla.2022.101344

http://hdl.handle.net/10138/353491
https://doi.org/10.1016/j.mtla.2022.101344

Journal Pre-proof

Effect of cascade overlap and C15 clusters on the damage evolution in Fe: An OKMC study

A. Esfandiarpour, J. Byggmästar, J.P. Balbuena, M.J. Caturla, K. Nordlund, F. Granberg

PII: S2589-1529(22)00031-X
DOI: https://doi.org/10.1016/j.mtla.2022.101344
Reference: MTLA 101344

To appear in: *Materialia*

Received date: 25 November 2021
Accepted date: 22 January 2022

Please cite this article as: A. Esfandiarpour, J. Byggmästar, J.P. Balbuena, M.J. Caturla, K. Nordlund, F. Granberg, Effect of cascade overlap and C15 clusters on the damage evolution in Fe: An OKMC study, *Materialia* (2022), doi: https://doi.org/10.1016/j.mtla.2022.101344

Graphical Abstract

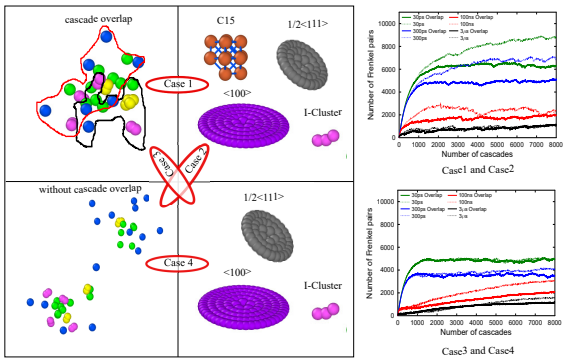

Case1 and Case2

Case3 and Case4

Effect of cascade overlap and C15 clusters on the damage evolution in Fe: An OKMC study

A. Esfandiarpour[a,b,*], J. Byggmästar[a], J. P. Balbuena[c], M. J. Caturla[c], K. Nordlund[a], F. Granberg[a]

[a] *Department of Physics, P.O. Box 43, FIN-00014 University of Helsinki, Finland*
[b] *NOMATEN Center of Excellence, National Centre for Nuclear Research, st. Andrzeja Soltana 7, 05-400, Otwock, Swierk, Poland*
[c] *Departamento de Fisica Aplicada, Universidad de Alicante, E-03690, Alicante, Spain*

Abstract

In order to investigate the long-term evolution of radiation-induced defects in the fission- and fusion-relevant material iron, we introduce cascade overlap effects into Object Kinetic Monte Carlo simulations. In addition to cascade overlap, we study the effect of introducing discrete C15 Laves phase clusters into the simulations. By applying either, none, or both of these effects we identify how they influence the evolution of the system. We find that both cascade overlap and C15 clusters affect the evolution of the radiation damage in different ways and on different time scales. Cascade overlap is found to reduce the number of Frenkel pairs. On the other hand, the explicit consideration of C15 Laves phase clusters increases the accumulation of defects at low dose. The results are compared to Molecular Dynamics simulation results under similar conditions.

Keywords: Cascade overlap, Object Kinetic Monte Carlo, Radiation damage, Iron, C15 clusters,

1. Introduction

Iron alloys are widely used in current nuclear power plants and are also proposed to be used in future ones as structural materials. The harsh environment in the form of elevated temperatures and continuous irradiation will degrade the material over time. This has led to extensive research focusing on radiation damage in Fe and Fe-based alloys [1–23]. Experimental studies of radiation damage in iron have shown that the accumulation of defects depends on dose, dose rate, and temperature [1, 2]. In these studies, transmission electron microscopy (TEM) and positron annihilation spectroscopy (PAS) techniques were used to detect the defect number and defect structure. It has been shown that by increasing dose, the defect density will saturate [1, 2]. TEM studies showed that the density of visible defects increases with an increasing dose rate. It should be noted that due to the detection limit of TEM techniques, there are some features of radiation damage that cannot be observed. Since TEM is a diffraction-based technique, it has a very weak

*Corresponding author.
Email address: am.esfandiyarpour@gmail.com (A. Esfandiarpour)

sensitivity to vacancy-type defects, such as voids. The detection limit of TEM also causes dislocation loops smaller than 1 nm to become invisible. Vacancy densities can be measured by PAS, and has for instance been carried out on iron irradiated up to a few tenths of a dpa at room temperature [1]. These kinds of experiments can directly be compared with both MD and OKMC simulations.

Additionally, Molecular Dynamics (MD) simulations have been used for characterising primary damage caused by irradiation [3]. The defect production and defect evolution can be described up to nanosecond timescales with MD simulations. This method has been used to study both the damage produced in single cascades [4] as well as the effect of overlapping cascades [6, 24–26]. The latter has mainly been used to obtain higher doses, closer to the ones in both experiments and in nuclear reactors. The main drawback of MD simulations is the limited timescale reachable, which is due to the simulation of discrete atoms and the simulation of the full trajectories of all atoms. Single impact simulations have revealed how the primary damage created is dependent on PKA energy, alloy composition, choice of interatomic potential and temperature [4, 24]. Additionally, the clustering and the spatial distribution of the created defects have been studied [4]. The cumulative irradiation studies have revealed how the defect number, the defect cluster size distribution and dislocation networks evolve as a function of dose [5–7].

To follow the evolution of defects induced by displacement cascade simulations on a longer time scale, several different Kinetic Monte Carlo (KMC) methods have been developed [8, 27–29]. Object Kinetic Monte Carlo (OKMC) is one of these methods and can simulate annealing of defects on extended time scales [9, 29, 30]. In this method, each defect is considered as an object. In iron these objects include single interstitials, single vacancies, interstitial clusters, vacancy clusters, voids, $1/2\langle 1\,1\,1\rangle$ loops, $\langle 1\,0\,0\rangle$ loops and C15 Laves phase clusters. These objects can migrate, dissociate, and interact with each other. Several OKMC simulations have been carried out on radiation damage in Fe and Fe-alloys [9–11, 29, 30]. These studies show how parameters related to defect properties and their interactions affect the evolution of the system. For example, formation of $\langle 1\,0\,0\rangle$ loops during irradiation of Fe was the main topic of a recent study [9]. The formation of $\langle 1\,0\,0\rangle$ loops is possible via different mechanisms, 1) interaction of two $1/2\langle 1\,1\,1\rangle$ loops [12] and 2) collapse of C15 clusters [7, 13]. Comparison of experimental results and OKMC simulation results utilising both mechanisms suggested that the most probable mechanism is the latter one. However, the effect of the presence of discrete C15 clusters in OKMC simulations and the effect of cascade overlap on the defect evolution in iron have not yet been studied.

The migration and formation energies of each object are the two most important parameters in OKMC simulations. DFT calculations can provide accurate data for point defects and small defect clusters, while the calculation of migration energies of large defect clusters is not usually possible due to computational limitations of this method. However, to calculate the formation energies of large clusters, recently ab initio accurate models have been developed [14]. Molecular Dynamics and Molecular Statics simulations are other sources used to obtain input parameters for OKMC simulations. These include defect structure, defect

morphology and spatial distribution of defects as a result of a collision cascade. Additionally, formation and migration energies of defect clusters, interactions between defects, and interaction between cascades and defects can be obtained from MD. The interaction between pre-existing debris and a nearby collision cascade is important when we want to investigate the evolution of materials under continuous irradiation. In iron and tungsten this interaction has been investigated in several studies [15, 16, 31]. It was found that the effect of a collision cascade in the vicinity of pre-existing defects and defect clusters will depend on the separation distance between them. For instance, the number of surviving point defects depends dramatically on this distance. It was observed that cascade overlap can completely change the defect morphology of interstitial clusters, e.g. change the Burgers vector of a dislocation loop [17]. In the same studies for iron, it was shown that the effect of interaction between cascades and pre-existing vacancy type clusters was not as significant [16].

In this study, we use OKMC simulations to study the evolution of radiation-induced defects in the fission- and fusion-relevant model material iron. To keep the atomistic accuracy of Molecular Dynamics, we have, in addition to what previous OKMC studies have incorporated, added the results of cascade overlap effects and effect of C15 Laves phase cluster formation. The former is based on MD results of cascades overlapping with pre-existing defects. We simulate different relaxation times between collision cascades, from very short times comparable with MD simulations, up to longer relaxation times more comparable to experiments. We investigate how both cascade overlap and C15 Laves phase clusters formation affect the evolution, by applying them individually and with both turned on and off.

2. Methods

OKMC simulations were carried out with the MMonCa code [30]. The migration and binding energies of each object larger than four defects are listed in Table 1. Formation and migration energies of interstitial type defects up to the size of 4 was extracted from DFT calculations [18]. Formation energy of dislocation loops and C15 clusters were the ones based on DFT in Ref. 14. For diffusion of $1/2\langle 1\,1\,1\rangle$ loops, molecular dynamics data was used [19]. The binding energy of defect clusters with sizes larger than 4, was calculated as $E_\mathrm{b} = E_\mathrm{f}(n-1) + E_\mathrm{f}(1) - E_\mathrm{f}(n)$, where n is the number of defects in the cluster. Using recent DFT-based formation energies of interstitial clusters [14] and values from Ref. 20 for vacancies in the above-mentioned equation, the binding energies were obtained (also presented in Table 1). In OKMC simulations, objects interact with each other if they are located within a certain capture radius. The capture radius between interstitials was between the third and the fourth nearest neighbor and the capture radius between vacancies was between the second and the third nearest neighbor. The capture radius between vacancies and interstitials was $1.9a_0$, where a_0 is the lattice constant [21].

The new implementation of cascade overlap was extracted from Ref. 15. This paper describes the interaction between cascades and pre-existing interstitial-type clusters. The effect of cascade overlap with

vacancy-type defect clusters was not included in this study, as the effect was found to not be as considerable as for interstitial-type clusters [16]. The number of new Frenkel pairs (FPs) created in the close vicinity of a pre-existing cluster was presented by an analytical model [15]. This model shows that the number of new Frenkel pairs decreases as the distance between the center of the cascade and the pre-existing cluster is less than a critical value, given by the size of the cluster and the cascade core. When cascade overlap happens, the probability of forming various types of self-interstitial clusters with certain size depends primarily on the relative formation energies of the different cluster types predicted by the used interatomic potential. We have used the probabilities found in Figures 15 and 16 in Ref. 15, one set which correspond to the interaction in the AM04 interatomic potential [22] and the other set to the M07-B interatomic potential [5, 23].

To introduce a new cascade to our simulation cell, we used the resulting debris of 50 single cascades from MD simulations with a 5 keV PKA energy. Each cascade insertion to the OKMC simulation box was randomly chosen. Before each cascade insertion, the system was evolved up to a predefined evolution time. Here, we considered four evolution times: 30 ps, 300 ps, 100 ns, and 3 μs at room temperature (300 K). The 30 ps evolution time is directly comparable with MD simulations of massively overlapping cascades [5–7]. When a new cascade was inserted, the distance between the cascade and the pre-existing interstitial clusters was calculated. If the separation distance was within the interaction range, the overlap effect was applied. The box size, 20 by 20 by 20 nm^3, is comparable with previous MD simulations of overlapping cascades. Periodic boundary conditions were applied in all three dimensions. The evolution of the systems was followed for up to 8 000 inserted cascades, which represent a dose of about 0.37 dpa. Fifteen simulations for each different case were carried out to obtain statistically significant results. The dose was calculated based on deposited energy in the system by each cascade. The number of displacements (N_d) induced by each cascade can be calculated based on the NRT-dpa equation [32]:

$$N_\mathrm{d} = 0.8T_\mathrm{d}/2E_\mathrm{d},$$

where E_d is the threshold displacement energy and T_d is the damage energy which can be calculated as $T_\mathrm{d} = E_\mathrm{PKA} - E_\mathrm{ES}$, where E_ES is the energy that is lost by electronic stopping. The number of displaced atoms induced by cascades divided by the number of total atoms (N_atom) can be considered as the dose. The relation between the number of cascades N_c and the dose can be calculated as follows:

$$\mathrm{Dose} = 0.8N_\mathrm{c}(E_\mathrm{PKA} - E_\mathrm{ES})/(2E_\mathrm{d}N_\mathrm{atom}).$$

The parameters T_d and E_ES were obtained from full MD simulations, E_d was 40 eV and N_atom the total number of atoms in the simulation cell.

To investigate the evolution of the system in OKMC, we consider two scenarios:

1. C15 laves phase clusters are directly included. Based on DFT calculations, C15 clusters are the most stable interstitial cluster up to sizes of around 50 interstitial atoms [14]. Larger than this size, the $1/2\langle 1\,1\,1\rangle$ loop becomes the most stable interstitial cluster. Molecular dynamics studies have shown

that by growing C15 up to a critical size, it collapses into $1/2\langle 1\,1\,1\rangle$ loops with a high probability and into $\langle 1\,0\,0\rangle$ loops with a low probability [7]. Based on these studies, we have considered the following model for inserting C15 clusters in OKMC simulations. When the numbers of interstitials in clusters become five, they transform to C15 clusters with a 70% probability and to $1/2\langle 1\,1\,1\rangle$ loops with a 30% probability. When the number of interstitials in a C15 cluster reaches 50, it will transform to a $\langle 1\,0\,0\rangle$ loop with a 5% probability and with a 95% probability to a $1/2\langle 1\,1\,1\rangle$ loop [7]. The shape of the C15 cluster was approximated by a sphere and the cluster was considered immobile. The atomic density of 3.5×10^{22} cm^{-3} was used for C15 clusters, which is similar to the density of them in MD simulations.

2. C15 was indirectly included in the simulations, similar to the nucleation model used in Ref. 9. In this scenario interstitial clusters with a size of 5 interstitials transform to $1/2\langle 1\,1\,1\rangle$ loops with a 95% probability and to $\langle 1\,0\,0\rangle$ loops with a 5% probability, skipping the intermediate step of C15 creation.

In both scenarios single interstitials and interstitial clusters of sizes up to 4 are mobile.

As the overlap effect depends on choice of interatomic potential, for the first scenario (with discrete C15) we employed the result from the M07-B potential, showing stable C15 clusters. For the second scenario (indirect C15 cluster effects) the result from the AM04 potential was used, where C15 is not stable. In order to investigate how cascade overlap affects the defect evolution in OKMC, we conducted two series of simulations. In the first series, cascade overlap effects are not imposed and in the other series the overlap effects are applied.

Defect Cluster	Binding energy (eV)	Migration barrier (eV)
C15 cluster ($I_{5\leq n<50}$)	$2.42 - 0.45(n^{2/3} - (n-1))^{2/3})$	immobile
$1/2\langle 1\,1\,1\rangle$ loop ($I_{n\geq 5}$)	$3.77 - 1.60(\sqrt{n}\ln n - \sqrt{n-1}\ln(n-1)) - 5.35(\sqrt{n} - \sqrt{n-1})$	0.05
$\langle 1\,0\,0\rangle$ loop ($I_{n\geq 5}$)	$3.77 - 1.78(\sqrt{n}\ln n - \sqrt{n-1}\ln(n-1)) - 7.16(\sqrt{n} - \sqrt{n-1})$	immobile
Vacancy cluster ($V_{n\geq 5}$)	$2.07 - 2.59(n^{2/3} - (n-1))^{2/3})$	immobile

Table 1: Binding energy (eV) and migration barrier (eV) of defect clusters with sizes larger than $n = 4$ interstitials (I) or vacancies (V).

3. Results

We categorize our simulations into four cases:

- *Case 1*: C15 is considered directly and overlap effects are turned on.
- *Case 2*: C15 is considered directly and overlap effects are turned off.
- *Case 3*: C15 effects are considered indirectly and overlap effects are turned on.
- *Case 4*: C15 effects are considered indirectly and overlap effects are turned off.

The results are shown in Figs. 1(a) and 1(b), for direct and indirect consideration of C15, respectively. In both figures the effect of overlap are visible in the number of Frenkel pairs. Fig. 1(a) compares *Case 1* and *Case 2* for four annealing times between each cascade and shows that the overlap effect decreases the number of surviving Frenkel pairs, especially at shorter relaxation times. We observe that the overlap effect is minimal when the relaxation time is 3 μs. Fig. 1(b) compares *Case 3* and *Case 4* for four annealing times between each cascade and we notice that the effect is opposite to *Case 1* and *Case 2*. Without explicit C15 the overlap effect is minute at short relaxation times, but great at the longer relaxation times. As we observe an effect of cascade overlap, we looked at the number of overlap events (cascades close to previous debris) as a function of number of cascades, shown in Fig. 2. We clearly see that direct consideration of C15 will increase the number of overlap events. Another trend seen is that a longer relaxation time will decrease the number of overlap events.

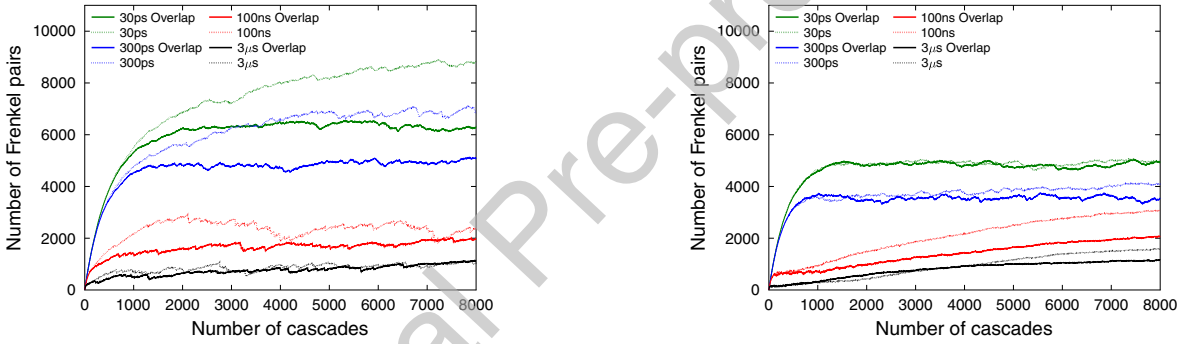

(a) *Case 1* and *Case 2*

(b) *Case 3* and *Case 4*

Figure 1: Number of Frenkel pairs as a function of number of cascades for (a) *Case 1* and *Case 2*, explicit C15 and with and without cascade overlap and (b) *Case 3* and *Case 4*, indirect C15 and with and without cascade overlap. The differences between different annealing times and cascade overlap effects are shown.

In Fig. 3 a comparison of the mean number of Frenkel pairs as a function of number of cascades for *Case 1* and *Case 3* is shown. We observe that formation of discrete C15 during cascade overlap simulations affects the results. At low dose, considering C15 directly increases the number of Frenkel pairs for all relaxation times. For longer relaxation times, the effect of C15 on the number of surviving FPs is smaller. To interpret this behavior, we analyzed the number of interstitials in C15 clusters, $\langle 1\,0\,0\rangle$, and $1/2\langle 1\,1\,1\rangle$ loops for two different annealing times, shown in Fig. 4. Due to the low migration barrier of $1/2\langle 1\,1\,1\rangle$ loops, they can easily be annealed through combination with vacancy clusters. C15 clusters and $\langle 1\,0\,0\rangle$ loops are immobile and play important roles in the accumulation of defects. In *Case 3*, $\langle 1\,0\,0\rangle$ loops are the only immobile interstitial-type cluster in the box, while for *Case 1* both C15 clusters and $\langle 1\,0\,0\rangle$ loops are present and immobile. Fig. 4 shows that by increasing the number of cascades (dose) the concentration of immobile

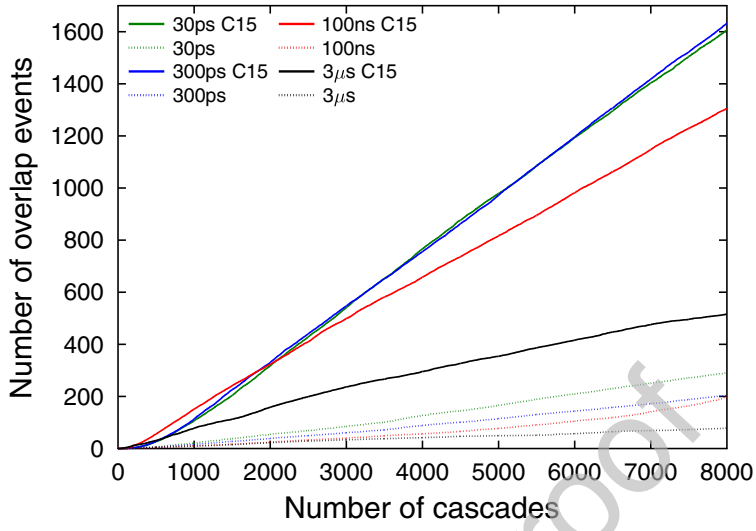

Figure 2: Number of overlap events as a function of number of cascades for different annealing times, when C15 is explicitly and indirectly considered.

clusters approach each other.

Looking at Figs. 1 and 3, we observe two general trends 1) Saturation in number of FPs is happening in all cases and setups; 2) By decreasing the evolution time between cascades (equivalent to increasing the dose rate) the number of residual defects increases. Results from MD simulations with the same time and size scale exist and the data from Figure 9 in Ref. 5 is plotted in Fig. 5. The MD simulation was carried out with the M07-B potential, which shows stable small C15 clusters. The relaxation time in the MD simulations was 30 ps. The OKMC results from this study, *Case 1*, with a relaxation time of 100 ns is shown in the same graph.

Fig. 6 shows the evolution of the microstructure in the OKMC simulations at various doses. In this figure we see the formation of point defects at low doses, and the defect accumulation and loop formation at higher doses. By increasing the dose, the number and the size of C15 clusters increase and the increase in size continues until C15 reaches its unstable size (50 interstitials) and collapse into $\langle 1\,0\,0\rangle$ and $1/2\langle 1\,1\,1\rangle$ loops. The $1/2\langle 1\,1\,1\rangle$ loops recombine with vacancies very quickly, while $\langle 1\,0\,0\rangle$ loops continue to grow.

Fig. 7 shows the mean density of vacancies for all cases at various doses in log-log scale. Saturation of vacancies can be seen for most cases at high dose, previously seen for the same data in Fig. 1. However, this figure highlights the intermediate steps not clearly visible in Fig. 1.

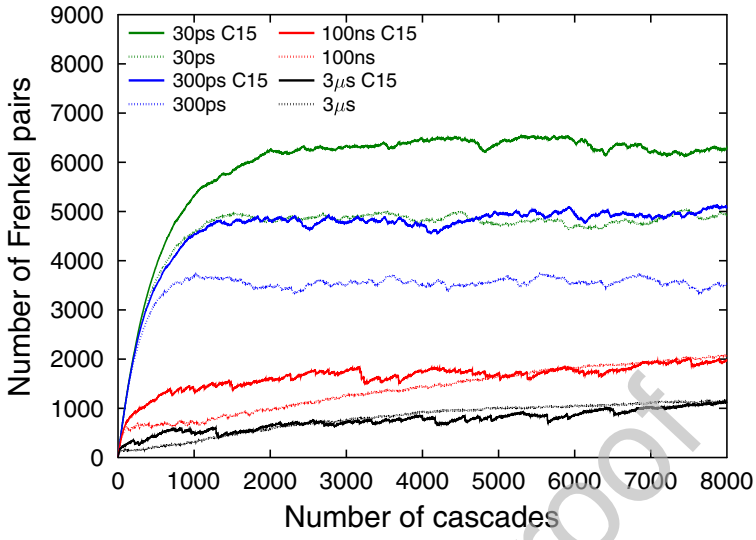

Figure 3: Comparison of number of Frenkel pairs as a function of number of cascades between the cases where C15 is explicitly and indirectly considered. Overlap effects are taken into account.

4. Discussion

In order to interpret the result of the overlap effect (Fig. 1(a) and Fig. 1(b)) we need to return to the analytical model for the interaction between single cascades and pre-existing clusters [15]. In this model, if the distance between the center of the cascade and the pre-existing cluster is below a certain value, the number of new Frenkel pairs produced is decreased. The type of the pre-existing cluster can also change, depending mainly on the relative formation energies of the different cluster types. In addition, to be able to investigate the overlap effect on defect morphology evolution, the number of surviving Frenkel pairs when overlap effects are turned on and off can be determined. Fig. 1(a) and Fig. 1(b) show that the overlap effect decreases the number of surviving Frenkel pairs. The reason for this decrease can be discussed as follows.

When C15 clusters are considered directly, a decreasing number of surviving Frenkel pairs is observed (Fig. 1(a)). The main reason of this decreasing trend is the lower number of new produced Frenkel pairs. In this case, the C15 clusters are immobile and cascade overlap will happen with a higher probability. By increasing the number of inserted cascades, the density of C15 in the box will increase and thus the probability of overlap will further increase. Fig. 2 shows the overlap events as a function of number of inserted cascades, which in this case increases dramatically.

When C15 clusters are not considered directly, the number of overlap events are fewer than in the case when C15 clusters are considered directly (Fig. 2). We see from Fig. 1(b), that after a certain dose, depending on annealing time, the overlap effect dominates. In this case, the density of immobile clusters (read $\langle 1\,0\,0 \rangle$

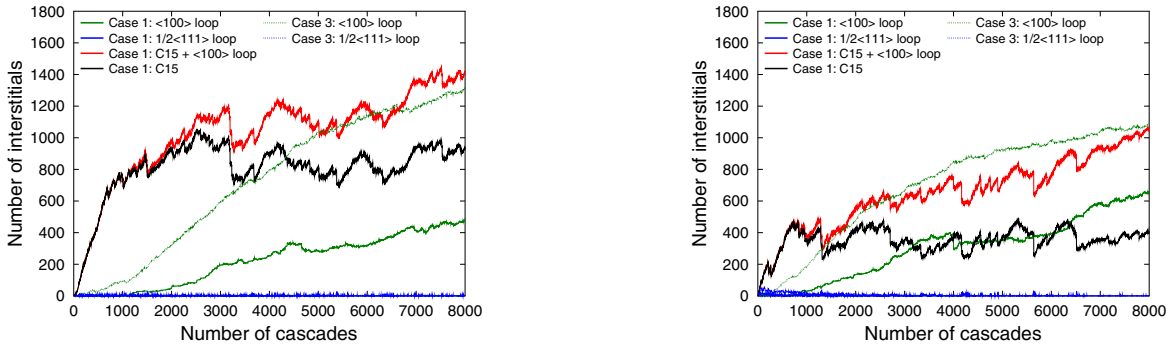

(a) 100 ns

(b) 3 μs

Figure 4: Comparison of the mean number of interstitials in mobile and immobile clusters as a function of number of cascades between the cases where C15 is explicitly and indirectly considered. The annealing time between each cascade is 100 nanoseconds (a) and 3 μs (b).

loops) determines the behavior, as the $\langle 1\,0\,0 \rangle$ loops behave as defect sinks. In addition to the decline in number of new Frenkel pairs produced due to overlap effects, change of Burgers vector of $\langle 1\,0\,0 \rangle$ loops by cascade overlap is the main source to the different behaviour between the cases with overlap effects turned on and off (Fig. 1(b)). Figure 15a in Ref. 15 shows that the there is a high probability of changing Burgers vector of pre-existing $\langle 1\,0\,0 \rangle$ loops up to sizes of 30 SIAs during cascade overlap. Hence, overlap effects decrease the concentration of surviving $\langle 1\,0\,0 \rangle$ loops and thus reduce the number of accumulated Frenkel pairs, as the mobile $1/2\langle 1\,1\,1 \rangle$ loops can recombine with vacancies.

Up to a certain number of cascades (Fig. 3), the number of Frenkel pairs in the case where C15 was not considered directly is lower than when it was considered directly, when overlap effects are considered. The reason for this difference goes back to the mobility of clusters that form during the cascade simulations. In the case where the intermediate stage of C15 formation is neglected (*Case 3*), $1/2\langle 1\,1\,1 \rangle$ loops with low migration barrier are formed instead of immobile C15. Thus, the recombination rate of interstitials with vacancies increases and the number of Frenkel pairs in the box decreases. The immobile interstitial defects such as $\langle 1\,0\,0 \rangle$ loops and C15 clusters are the source of defect accumulation. Fig. 4 describes how the number of interstitials in immobile clusters in *Case 3* approaches the ones in *Case 1*.

For a similar setup, both MD and OKMC (*Case 1*), show a very similar trend in terms of number of Frenkel pairs (Fig. 5). In MD simulations, the M07-B interatomic potential had been used, which shows stable C15 clusters corresponding to *Case 1*. However, to obtain comparable results, the annealing time between each cascade is different between MD simulations (30 ps) and OKMC simulations (100 ns). The attempt frequency is on the order of 10^{13} s^{-1}, based on the Bortz-Kalos-Liebowitz (BKL) algorithm used for calculating evolution time in OKMC, which results in not many reactions occurring on the timescale of

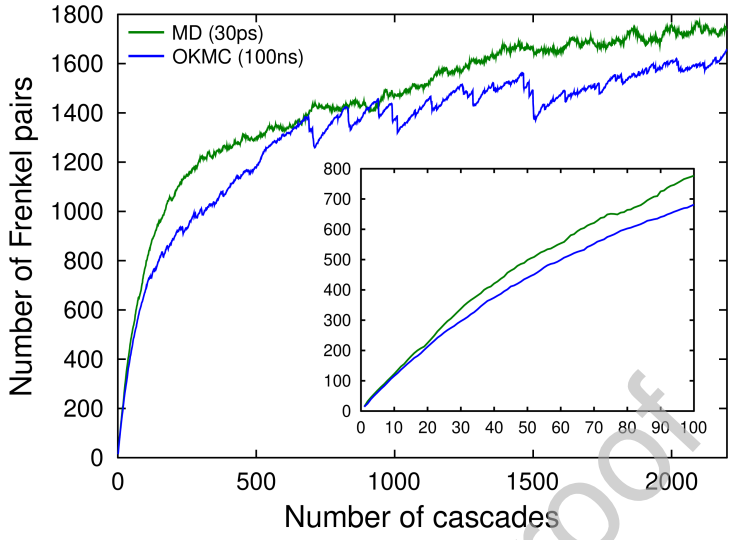

Figure 5: Comparison of Frenkel pairs as a function of number of cascades in MD [6] and OKMC simulations. In the MD simulations the annealing time between each cascade is 30 ps, while in OKMC simulation the annealing time is 100 ns. In the OKMC simulation both C15 and cascade overlap were considered. The inset is a zoom-in at the evolution up to 100 cascades.

picoseconds. This leads to accumulation of higher defect numbers in OKMC simulations when the annealing time between cascade is only on the order of tens of picoseconds. Another factor is the effects of elastic interactions, inherently accounted for in MD simulations, but not included in the current OKMC simulation. The elastic strain fields induced by the various defect clusters can change the migration barriers for nearby defects [33].

Generally, looking at the defect evolution in all simulations, we observe that there will be a build-up under all circumstances. Contrary to electron irradiation, where only point defects are produced, there would be almost no defect build-up at room temperature, as all defects would annihilate without any generic traps [34]. This shows that utilizing realistic cascade debris, not just the correct number of Frenkel pairs, is crucial for understanding the microstructure evolution.

Looking more closely at Fig. 7, we observe that for the longer relaxation times, the vacancy density seems to saturate at quite low doses, but starts to increase again at a bit higher doses. This is especially clear in the cases without discrete C15 clusters (*Case 3* and *Case 4*). The first saturation is due to the formation of mobile $1/2\langle 1\,1\,1\rangle$ loops that easily can annihilate other defects. This is not as clearly seen in the cases where we have a quite high amount of immobile C15 clusters. However, as the dose increases, we form immobile $\langle 1\,0\,0\rangle$ loops which do not recombine as easily with vacancies (which are also immobile). This formation of the immobile interstitial type defect clusters will dramatically increase the number of defects in the system (almost an order of magnitude). This shows the importance of the immobile C15 clusters on

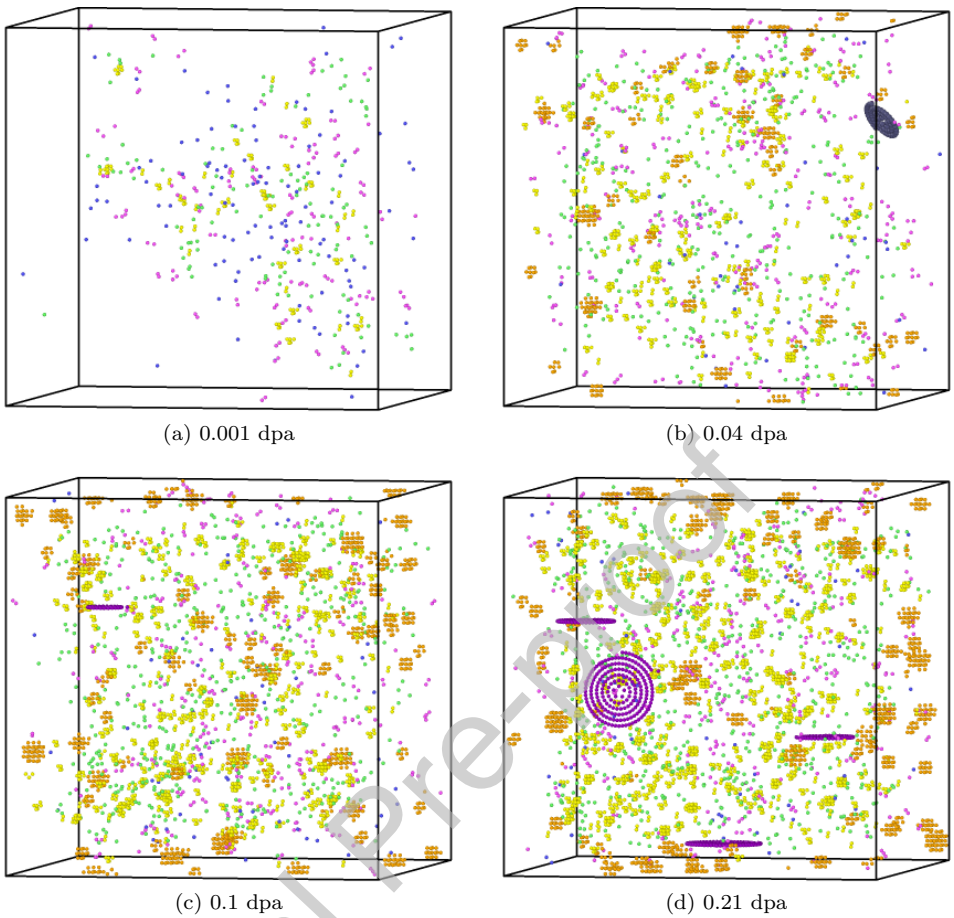

(a) 0.001 dpa (b) 0.04 dpa

(c) 0.1 dpa (d) 0.21 dpa

Figure 6: Snapshots of the OKMC simulation cell at various doses. In this figure both C15 and cascade overlap were considered and the relaxation time between cascades is 100ns. Green, blue, yellow, pink, orange, black and purple represent vacancies, interstitials, vacancy clusters, interstitial clusters (with size 2-4), C15 clusters, $1/2\langle 1\,1\,1\rangle$ loops and $\langle 1\,0\,0\rangle$ loops, respectively. The side length of the box is 20 nm.

the evolution, a similar trend was also seen in MD simulations [7].

5. Conclusions

Cascade simulations with four different annealing times have been performed by OKMC in this study. We implemented the effects of cascades overlapping with interstitial-type defect clusters in OKMC and studied the results with this implementation turned on and off. Additionally, we studied the evolution of defects during cascade simulations utilizing two different considerations of C15 Laves phase clusters. We have shown that both of these factors will affect the evolution of the system, both in terms of number of defects and defect morphology. Our summarized results and conclusions are the following:

1. Cascade overlap effects reduce the number of surviving Frenkel pairs.
2. The method of C15 Laves phase cluster consideration (direct or indirect) affects the results.

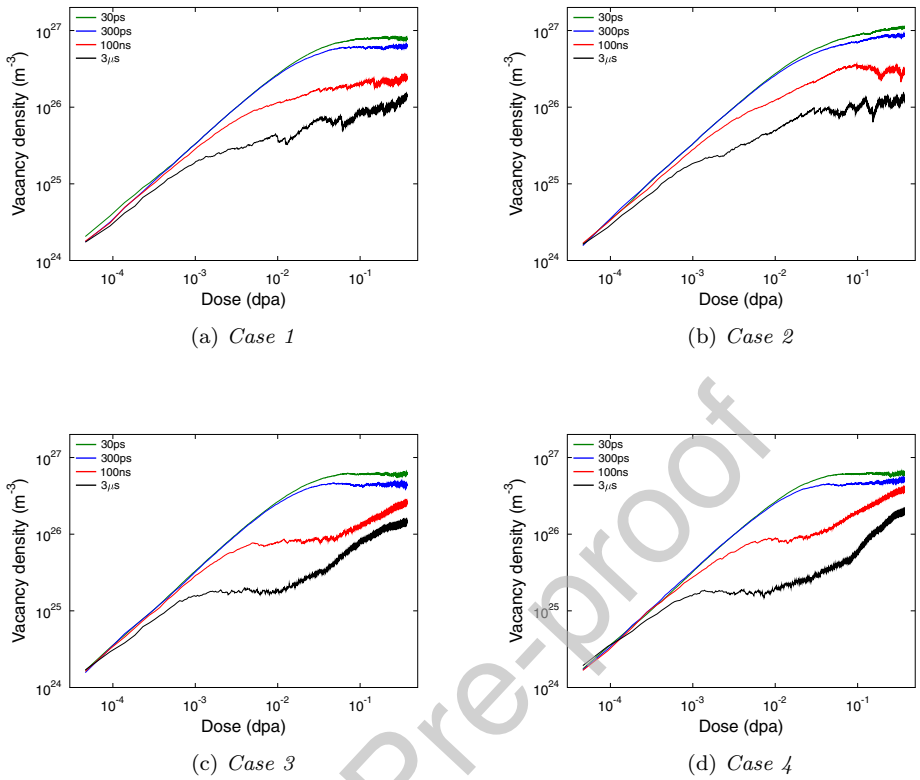

(a) *Case 1* (b) *Case 2*

(c) *Case 3* (d) *Case 4*

Figure 7: Vacancy density as a function of dose for all four cases at different annealing times in log–log scale.

- When considered directly, more defect accumulation is observed up to a certain dose and this dose depends on annealing time.
- The different considerations also changed the defect build-up mechanisms.

3. Saturation of the number of Frenkel pairs happens in all setups investigated.
4. By decreasing the evolution time between cascades (equivalent to increasing the dose rate) the number of residual defects increases.
5. When the same setup is considered in both MD and OKMC, the Frenkel pair evolution is qualitatively the same. The annealing time, however, needs to be different in the different methods to obtain quantitative agreement.

Acknowledgements

This work has been carried out within the framework of the EUROfusion Consortium and has received funding from the Euratom research and training programme 2014–2018 and 2019–2020 under grant agreement No 633053. The views and opinions expressed herein do not necessarily reflect those of the European

Commission. Grants of computer time from the IT Center for Science - CSC - Finland and Finnish Grid and Cloud Infrastructure (persistent identifier urn:nbn:fi:research-infras-2016072533) is gratefully acknowledged.

References

[1] M. Eldrup, B. N. Singh, Accumulation of point defects and their complexes in irradiated metals as studied by the use of positron annihilation spectroscopy–a brief review, J. Nucl. Mater. 323 (2–3) (2003) 346–353.

[2] R. Schäublin, B. Décamps, A. Prokhodtseva, J. F. Löffler, On the origin of primary 1/2 a_0 $\langle 1\,1\,1\rangle$ and a_0 $\langle 1\,0\,0\rangle$ loops in irradiated Fe(Cr) alloys, Acta Mater. 133 (2017) 427–439.

[3] K. Nordlund, S. J. Zinkle, A. E. Sand, F. Granberg, R. S. Averback, R. E. Stoller, T. Suzudo, L. Malerba, F. Banhart, W. J. Weber, F. Willaime, S. L. Dudarev, D. Simeone, Primary radiation damage: A review of current understanding and models, J. Nucl. Mater. 512 (2018) 450–479.

[4] C. Björkas, K. Nordlund, Comparative study of cascade damage in Fe simulated with recent potentials, Nucl. Instr. Meth. Phys. Res. Sec. B. 259 (2) (2007) 853–860.

[5] J. Byggmästar, F. Granberg, K. Nordlund, Effects of the short-range repulsive potential on cascade damage in iron, J. Nucl. Mater. 508 (2018) 530–539.

[6] F. Granberg, J. Byggmästar, K. Nordlund, Defect accumulation and evolution during prolonged irradiation of Fe and FeCr alloys, J. Nucl. Mater. 528 (2020) 151843.

[7] J. Byggmästar, F. Granberg, Dynamical stability of radiation-induced C15 clusters in iron, J. Nucl. Mater. 528 (2020) 151893.

[8] C. Björkas, K. Nordlund, M. J. Caturla, Influence of the picosecond defect distribution on damage accumulation in irradiated α-Fe, Phys. Rev. B 85 (2) (2012) 024105.

[9] J. P. Balbuena, M. J. Aliaga, I. Dopico, M. Hernández-Mayoral, L. Malerba, I. Martin-Bragado, M. J. Caturla, Insights from atomistic models on loop nucleation and growth in α-Fe thin films under Fe+ 100 keV irradiation, J. Nucl. Mater. 521 (2019) 71–80.

[10] L. Gámez, B. Gámez, M. J. Caturla, D. Terentyev, J. M. Perlado, Object kinetic Monte Carlo calculations of irradiated Fe–Cr dilute alloys: The effect of the interaction radius between substitutional Cr and self-interstitial Fe, Nucl. Instr. Meth. Phys. Res. Sec. B. 269 (14) (2011) 1684–1688.

[11] D. Terentyev, I. Martin-Bragado, Evolution of dislocation loops in iron under irradiation: The impact of carbon, Scr. Mater. 97 (2015) 5–8.

[12] H. Xu, R. E. Stoller, Y. N. Osetsky, D. Terentyev, et al., Solving the puzzle of $\langle 1\,0\,0\rangle$ interstitial loop formation in bcc iron, Physical review letters 110 (26) (2013) 265503.

[13] Y. Zhang, X.-M. Bai, M. R. Tonks, S. B. Biner, Formation of prismatic loops from C15 laves phase interstitial clusters in body-centered cubic iron, Scripta materialia 98 (2015) 5–8.

[14] R. Alexander, M. C. Marinica, L. Proville, F. Willaime, K. Arakawa, M. R. Gilbert, S. L. Dudarev, Ab initio scaling laws for the formation energy of nanosized interstitial defect clusters in iron, tungsten, and vanadium, Phys. Rev. B 94 (2) (2016) 024103.

[15] J. Byggmästar, F. Granberg, A. E. Sand, A. Pirttikoski, R. Alexander, M. C. Marinica, K. Nordlund, Collision cascades overlapping with self-interstitial defect clusters in Fe and W, J. Phys.: Condens. Matter 31 (24) (2019) 245402.

[16] F. Granberg, J. Byggmästar, K. Nordlund, Cascade overlap with vacancy-type defects in Fe, Eur. Phys. J. B 92 (7) (2019) 146.

[17] F. Granberg, J. Byggmästar, A. E. Sand, K. Nordlund, Cascade debris overlap mechanism of $\langle 1\,0\,0\rangle$ dislocation loop formation in Fe and FeCr, EPL (Europhysics Letters) 119 (5) (2017) 56003.

[18] C. C. Fu, J. Dalla Torre, F. Willaime, J. L. Bocquet, A. Barbu, Multiscale modelling of defect kinetics in irradiated iron, Nature Mater. 4 (1) (2005) 68–74.

[19] N. Soneda, T. Diaz de La Rubia, Migration kinetics of the self-interstitial atom and its clusters in bcc Fe, Phil. Mag. A 81 (2) (2001) 331–343.

[20] N. Soneda, T. Diaz de la Rubia, Defect production, annealing kinetics and damage evolution in α-Fe: An atomic-scale computer simulation, Phil. Mag. A 78 (5) (1998) 995–1019.

[21] F. Gao, D. J. Bacon, A. V. Barashev, H. L. Heinisch, Kinetic Monte Carlo annealing simulation of damage produced by cascades in alpha-iron, MRS Proceedings 540 (1998) 703.

[22] G. J. Ackland, M. I. Mendelev, D. J. Srolovitz, S. Han, A. V. Barashev, Development of an interatomic potential for phosphorus impurities in α-iron, J. Phys.: Condens. Matter 16 (27) (2004) S2629–S2642.

[23] M.-C. Marinica, F. Willaime, J.-P. Crocombette, Irradiation-induced formation of nanocrystallites with C15 laves phase structure in bcc iron, Physical review letters 108 (2) (2012) 025501.

[24] K. Vörtler, C. Björkas, D. Terentyev, L. Malerba, K. Nordlund, The effect of Cr concentration on radiation damage in FeCr alloys, J. Nucl, Mater. 382 (1) (2008) 24–30.

[25] F. Granberg, K. Nordlund, M. W. Ullah, K. Jin, C. Lu, H. Bei, L. M. Wang, F. Djurabekova, W. J. Weber, Y. Zhang, Mechanism of radiation damage reduction in equiatomic multicomponent single phase alloys, Phys. Rev. Lett. 116 (2016) 135504.

[26] E. Levo, F. Granberg, C. Fridlund, K. Nordlund, F. Djurabekova, Radiation damage buildup and dislocation evolution in Ni and equiatomic multicomponent Ni-based alloys, J. Nucl. Mater. 490 (2017) 323–332.

[27] J. Dalla Torre, J. L. Bocquet, N. V. Doan, E. Adam, A. Barbu, Jerk, an event-based Kinetic Monte Carlo model to predict microstructure evolution of materials under irradiation, Phil. Mag. 85 (4–7) (2005) 549–558.

[28] T. Opplestrup, V. V. Bulatov, G. H. Gilmer, M. H. Kalos, B. Sadigh, First-passage Monte Carlo algorithm: diffusion without all the hops, Phys. Rev. Lett. 97 (23) (2006) 230602.
[29] C. S. Becquart, A. Souidi, C. Domain, M. Hou, L. Malerba, R. E. Stoller, Effect of displacement cascade structure and defect mobility on the growth of point defect clusters under irradiation, J. Nucl. Mater. 351 (1–3) (2006) 39–46.
[30] I. Martin-Bragado, A. Rivera, G. Valles, J. L. Gomez-Selles, M. J. Caturla, Mmonca: An object kinetic Monte Carlo simulator for damage irradiation evolution and defect diffusion, Comp. Phys. Commun. 184 (12) (2013) 2703–2710.
[31] A. Fellman, A. E. Sand, J. Byggmästar, K. Nordlund, Radiation damage in tungsten from cascade overlap with voids and vacancy clusters, J. Phys.: Condens. Matter 31 (40) (2019) 405402.
[32] A proposed method of calculating displacement dose rates, Nuclear Engineering and Design 33 (1) (1975) 50–54.
[33] P.-W. Ma, S. L. Dudarev, Effect of stress on vacancy formation and migration in body-centered-cubic metals, Phys. Rev. Materials 3 (6) (2019) 063601. doi:10.1103/PhysRevMaterials.3.063601.
[34] C. Domain, C. Becquart, L. Malerba, Simulation of radiation damage in fe alloys: an object kinetic monte carlo approach, J. Nucl. Mater. 335 (1) (2004) 121–145.

Declaration of interests

☒ The authors declare that they have no known competing financial interests or personal relationships that could have appeared to influence the work reported in this paper.

☐The authors declare the following financial interests/personal relationships which may be considered as potential competing interests: